FOLDING OF THE INTRINSICALLY DISORDERED PAR-4 TUMOR SUPPRESSOR UNDER NATIVE AND EXTREME CONDITIONS

Andrea M. Clark

Advisor: Dr. Steven M. Pascal

Department of Chemistry and Biochemistry, Old Dominion University

Abstract

Proteins are an essential component of life on earth. Interestingly, some proteins are well adapted to extreme conditions, such as those conditions found in extraterrestrial environments. These conditions include alkaline/acidic pH, extreme temperature, and high salt. In this study, circular dichroism (CD) spectroscopy, dynamic light scattering (DLS), fluorescence, and size exclusion chromatography with multi-angle light scattering (SEC-MALS) were used to characterize the structure and stability of cl-Par-4 in native and extreme conditions. Cl-Par-4 is the caspase-3-cleaved fragment of the Par-4 tumor suppressor that is capable of killing cancer cells.

We have found that the conformation of cl-Par-4 is stable only in extreme conditions of acidic pH or high salt, while physiological conditions actually promote aggregation and disorder. This trend is likely due to charge-charge repulsion in the coiled coil domain. Mutagenic analysis will confirm if coiled coil destabilization and electrostatic interactions are key to folding in extreme conditions. This research provides an opportunity to simultaneously characterize the structure of a medically relevant human tumor suppressor protein and additionally use Par-4 as a case study of protein folding in extreme conditions.

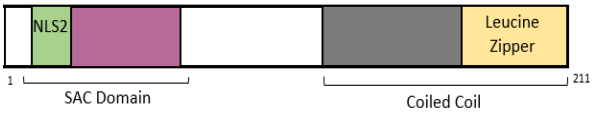

Figure 1. Domain structure of cl-Par-4.

Introduction

The amino acid glycine was found on the Murchison meteorite, indicating that these essential building blocks of life could potentially exist outside of earth. If proteins could exist outside of earth, we still do not know if they would fold differently in extraterrestrial environments. We seek to address this question by studying the structure of a human tumor suppressor protein that is stable in extreme conditions of high salt or acidic pH, which are similar to conditions in extraterrestrial environments.

This tumor suppressor is prostate apoptosis response-4 (Par-4). Par-4 has implications in both cancer and neurodegenerative disease [1, 2]. As a mostly intrinsically disordered protein (IDP), full length Par-4 does not form a fixed three-dimensional structure [3, 4]. Cleavage of Par-4 by caspase-3 generates an approximately 24 kilodalton fragment (cl-Par-4) [5] that is capable of nuclear translocation and inhibition of pro-survival genes like TOPO-1 and NF-ƙB. Figure 1 shows the domain structure of cl-Par-4 which has an N-terminal selective for apoptosis induction in cancer cells (SAC) domain with a nuclear localization signal (NLS2), a linker region, and a C-terminal coiled coil with a leucine zipper [6, 7]. Many binding interactions involving cl-Par-4 are mediated via the leucine zipper region. NLS2, located within the SAC domain, is important for nuclear import.

We have identified that the extreme conditions of (i) acidic pH (pH 4) or (ii) high salt (1 – 3 M NaCl) at neutral pH, each promote folding of cl-Par-4. Interestingly, environments with both high acidity and high salinity have been found on celestial bodies. It is thought that ancient Mars had a highly acidic environment. Jarosites, a family of minerals found on Mars, form at a highly acidic pH of 0 to 4 [8, 9]. Interestingly, cellular organelles like lysosomes, endosomes, and exosomes have an acidic pH that can potentially mimic an environment such as Mars [10]. Lysosomes have a pH as low as 4.5 and Par-4 can localize in exosomes which derive from the lysosome-endosome pathway [10-12]. Additionally, Saturn's moon Titan has high salinity, potentially similar to that of the Dead Sea on Earth. Therefore, studying the structure of Par-4 at both acidic pH and high salt will serve as a model of protein folding in extraterrestrial environments similar to that of celestial bodies like Mars or Titan, while also providing insight into its function in cells.

Additionally, throughout the course of evolution, some proteins on earth have adapted to life in extreme environments such as high salt [13, 14]. These halophilic proteins are influenced by electrostatic interactions and often form random coil structures, both common trends among intrinsically disordered proteins (IDPs) like Par-4. This suggests a possible link between halophilic protein adaption and IDP folding/structural flexibility [14]. Our mutagenic studies of Par-4 will identify if electrostatic interactions are key for stability in extreme environments. It is plausible that if proteins could exist outside of earth, they would have characteristics similar to IDPs, which encompass many medically relevant proteins.

Methods

This research project is divided into two aims: (1) characterize the structure of cl-Par-4 in native and extreme environments and (2) use site-directed mutagenesis to generate cl-Par-4 leucine zipper mutants.

In aim 1, cl-Par-4 was expressed in BL21(DE3) *E. coli* cells and purified according to published procedures using IMAC [15, 16]. The structure and stability of purified cl-Par-4 was characterized using circular dichroism (CD) spectroscopy, dynamic light scattering (DLS), intrinsic tyrosine fluorescence, and size exclusion chromatography with multi-angle light scattering (SEC-MALS). Results were obtained in native (physiological) conditions of 20 mM NaCl, 10 mM Tris-HCl, pH 7. Extreme conditions tested include 20 mM NaCl with a pH range of 4-10 encompassing both highly acidic and basic pH values. At neutral pH, extreme conditions of high salt up to 5 M NaCl were tested. Protein was at a concentration of 0.2 mg/mL for CD, DLS, and fluorescence measurements and at 3 mg/mL for SEC-MALS analysis.

In aim 2, primers for two full length Par-4 mutants were designed. Primer set 1 was designed to insert a lysine (K) in place of aspartic acid (D313) and primer set 2 was designed to insert a lysine in place of glutamic acid (E318). These mutants are D313K and E318K. After primers were designed, side directed mutagenesis was performed using codon optimized full length Par-4 as a template. The PCR product was purified using a Promega PCR clean up kit and transformed into DH5α *E. coli* cells using electroporation. Transformed culture was plated onto LB supplemented with 100 µg/mL ampicillin. Colonies were inoculated into LB with ampicillin and then the plasmid DNA was extracted. Three samples per mutation were sent for DNA sequencing. Results from showed wild type, not mutant DNA. Plasmid DNA from additional colonies will be extracted and sent for DNA sequencing to confirm the presence of the desired mutations.

Results and Discussion

I. Acidic pH-Induced Folding

The secondary structure of cl-Par-4 was investigated using CD spectroscopy. CD spectra of cl-Par-4 show increased helical content (approximately 80%) at pH 4, evident by intense dichroism around 222 and 208 nm (Figure 2a,b). Decreased helicity and increased disorder content was observed at pH 7 and 10. CD spectra obtained from 5 to 85 °C show increased thermal stability at acidic pH (Figure 2c) and decreased thermal stability at pH 7 (Figure 2d). This suggests acidic pH is necessary for folding into a predominantly alpha helical structure that has increased heat tolerance. Additionally, the isoelectric point (pI) significantly affects the degree of helical content and folding (Figure 2e,f). Helical content is greater below the pI of 5.4; however, helicity decreases at pH values above the pI where cl-Par-4 has a net negative charge.

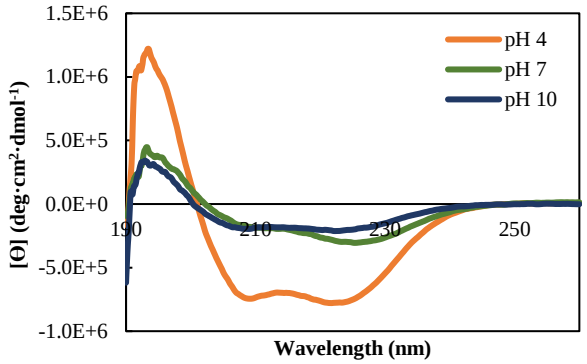

(a)

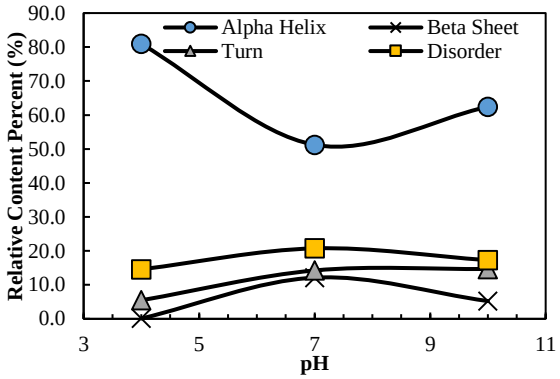

(b)

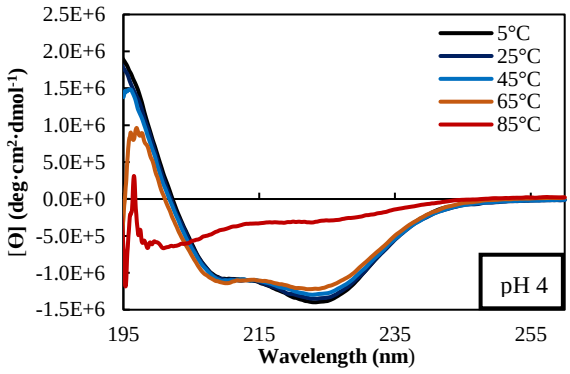

(c)

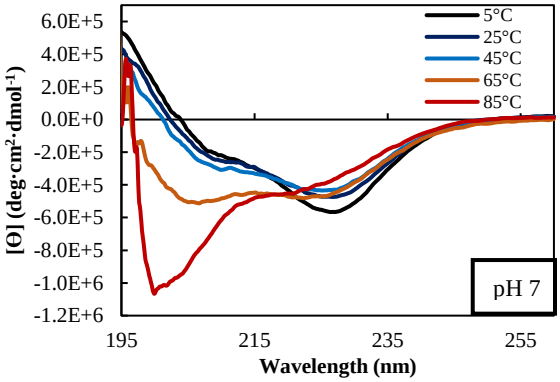

(d)

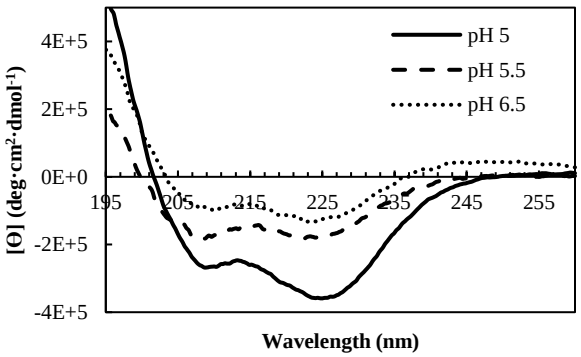

(e)

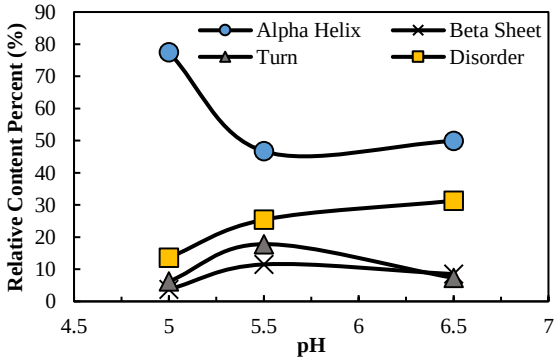

(f)

Figure 2. Circular dichroism of cl-Par-4 at varying pH conditions. (a) CD of cl-Par-4 in pH 4, 7, and 10 buffer. (b) Dependence of secondary structure content on pH. (c) Thermal stability in acidic pH. (d) Thermal stability in neutral pH. (e) CD below and above the pI (5.4). (f) Secondary structure below and above the pI.

Dynamic light scattering was used to investigate the effect of pH on the hydrodynamic size of cl-Par-4 (Figure 3a). The measured Stokes radius (R_s) values were 483 nm at pH 7, 339 nm at pH 10, and 43 nm at pH 4. The decrease in R_s as pH decreases indicates a more compact and folded structure at acidic pH, while aggregation occurs at pH 7 and 10. Zeta potential measurements gave an experimental pI of 5.35 which is close to the theoretical pI of 5.39. Significant aggregation occurs above the pI (Figure 3b), suggesting the pI plays an important role in the stability and self-association of cl-Par-4. Additionally, Figure 3c shows that in acidic pH, cl-Par-4 is much more stable over time. However, in pH 7 and 10, there is significant variation in hydrodynamic size over time. Therefore, not only does acidic pH increase helicity, but also decreases hydrodynamic size.

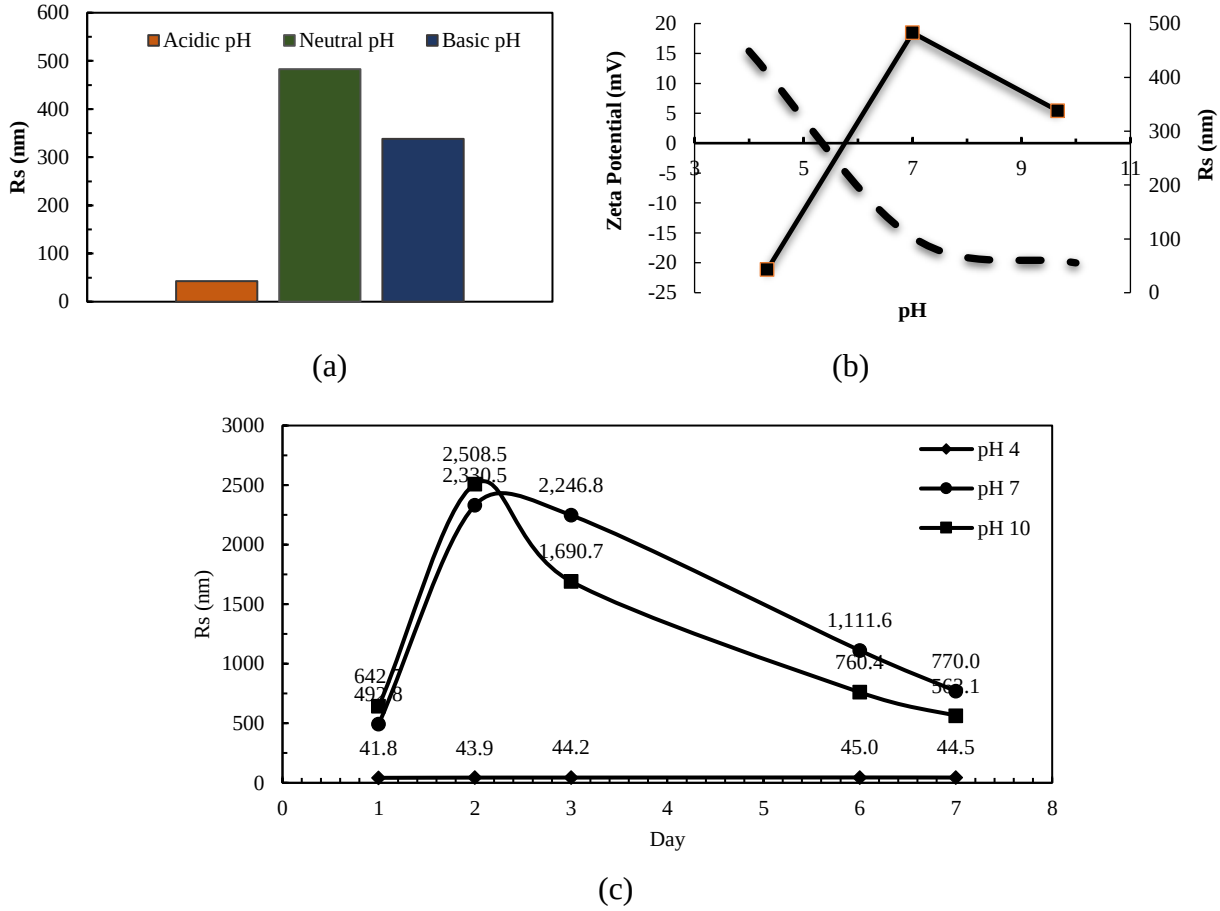

Figure 3. Dependence of hydrodynamic properties on pH (a) Measured Rs of cl-Par-4 under native and denaturing conditions by Dynamic Light Scattering (DLS). b) Relationship of zeta potential (dashed) to pH and Rs (solid line). (**c**) Measured Rs over seven days at pH 4, 7, and 10.

Intrinsic tyrosine fluorescence can be used to investigate protein tertiary structure. Cl-Par-4 has five tyrosine residues, one in the SAC and four in the linker region. Tyrosine was selectively excited at 220 nm and the emission spectra was recorded from 250-400 nm. The intensity of the fluorescence emission spectra is dependent upon the exposure of the aromatics to the polar solvent. Higher fluorescence intensity correlates to a better folded protein with aromatics buried within the core. Lower intensity correlates to increased solvent exposure and unfolding of the protein.

In acidic pH, the fluorescence intensity around 310 nm is higher than neutral pH (Figure 4a), and also shows better thermal stability (Figure 4b). This indicates that cl-Par-4 is predominantly folded in acidic pH, and that a disordered and aggregated structure predominates in physiological conditions.

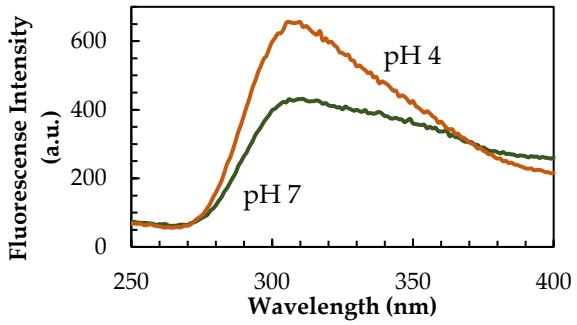

(a)

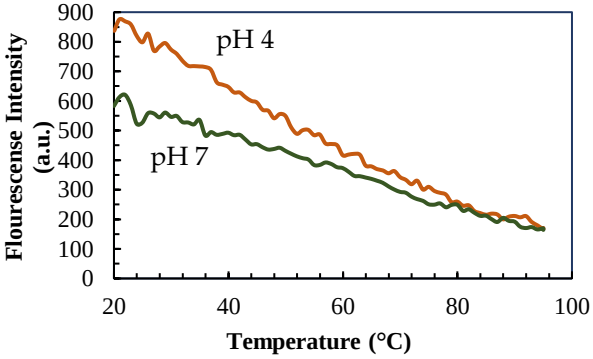

(b)

Figure 4. Increased tertiary structure at acidic pH. (a) Tyrosine fluorescence emission at pH 4 and 7. (b) Thermal stability measured by fluorescence emission at 310 nm at pH 4 and 7.

II. Tetramer formation in 1 M NaCl

The secondary structure of cl-Par-4 was also investigated in varying salt conditions ranging from 0.02-3 M NaCl, with 0.02-0.15 M representing physiological and greater than 0.25 M representing extreme salt conditions. Figure 5a shows increased helical content in high salt ranging from 0.35-3 M NaCl, while low salt produces a more disordered spectrum. Secondary structure analysis (Figure 5b) shows helicity increases with increased salt and disorder and beta content decrease.

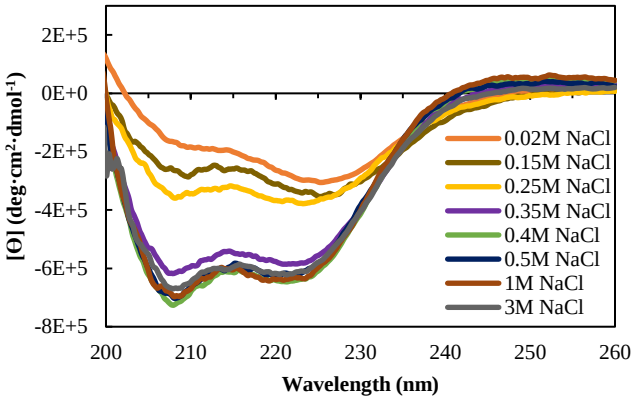

(a)

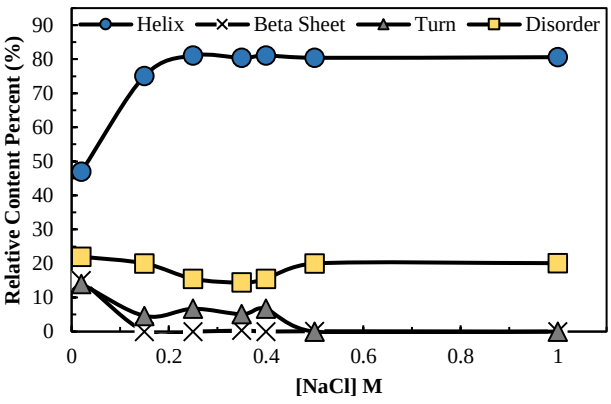

(b)

Figure 5. CD spectra of cl-Par-4 in varying salt conditions. (a) CD of cl-Par-4 in 0.02-3 M NaCl. (b) Dependence of secondary structure on NaCl concentration.

The dependence of hydrodynamic size on salt concentration was also investigated. Figure 6 shows large measured Rs values in low salt, characteristic of aggregation. However, high salt in the range of 0.5-1 M NaCl produces a smaller hydrodynamic size, consistent with a more compact, folded structure.

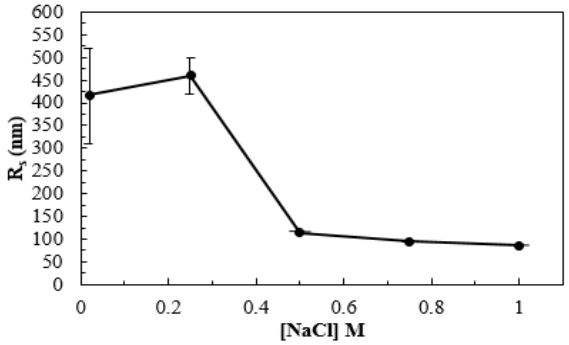

Figure 6. Decreased hydrodynamic size with increased ionic strength.

Intrinsic tyrosine fluorescence was used to determine the effect of ionic strength on tertiary structure (Figure 7). Higher emission in 1 M NaCl suggests a more folded structure compared to low salt. Decreased emission in low salt is consistent with a less folded structure.

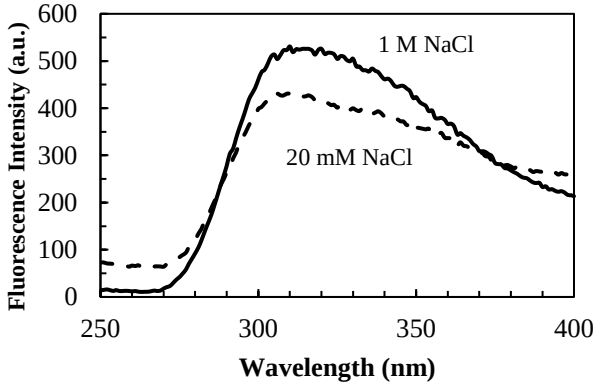

Figure 7. Tyrosine fluorescence in high and low salt.

SEC-MALS experiments were performed using a Superdex 200 gel filtration column to determine molar mass (MM) and size of the aggregates in low salt (0.02 M NaCl) and of the folded conformation in high salt (1 M NaCl). Light scattering (LS), UV, and refractive index (RI) measurements were obtained to determine MM.

SEC-MALS analysis in low salt showed a mixture of large aggregates (Table 1). The major peak eluted after 70 minutes and scattered light intensely, indicating a large molecular size (Figure 8a). MM measurements could not accurately be calculated for the small second and third peaks that eluted between 71-75 minutes. The major peak had an average MM of 389 kilodaltons (Table 1). However, plotting the elution profile as a function of MM shows variation in MM as the sample eluted from the column (Figure 8b), suggesting a somewhat heterogeneous sample. Since the MM of monomeric cl-Par-4 is 24 kilodaltons, the results are consistent with a primary species close to a 16mer, but other oligomers are likely present. The average R_g for this sample was 128 nm (Table 1).

When the SEC-MALS experiment was repeated with a second sample, also at low salt (0.2 mM NaCl), the fraction that eluted near 70 minutes had a somewhat larger MM of 517 kilodaltons, consistent with a 22mer (theoretical 22mer MM is 528 kilodaltons), and an R_g of 155 nm (Figure 8c, Table 1). In both low salt samples, individual MM measurements had an error in the range of 24-39%. Though these results are inexact, clearly, SEC-MALS consistently predicts higher-order oligomers in low salt, while the

presence of multiple peaks suggests multiple, possibly interconverting, aggregated species. This is not unexpected for a disordered protein which is highly flexible.

A double log conformation plot of MM versus radius provides protein shape information. A slope of 0.33 would indicate spherical, a slope of 0.5 would suggest coil, and a slope of 1 would suggest rod-like shape [17]. The conformation plot in Figure 8d shows slopes of 0.44 and 0.71. At least some of the difference between these two values is due to fitting uncertainty, since visually, the slopes of the two curves would appear to be more similar than these numbers suggest. But both of these slope values suggest at least some coil-like character.

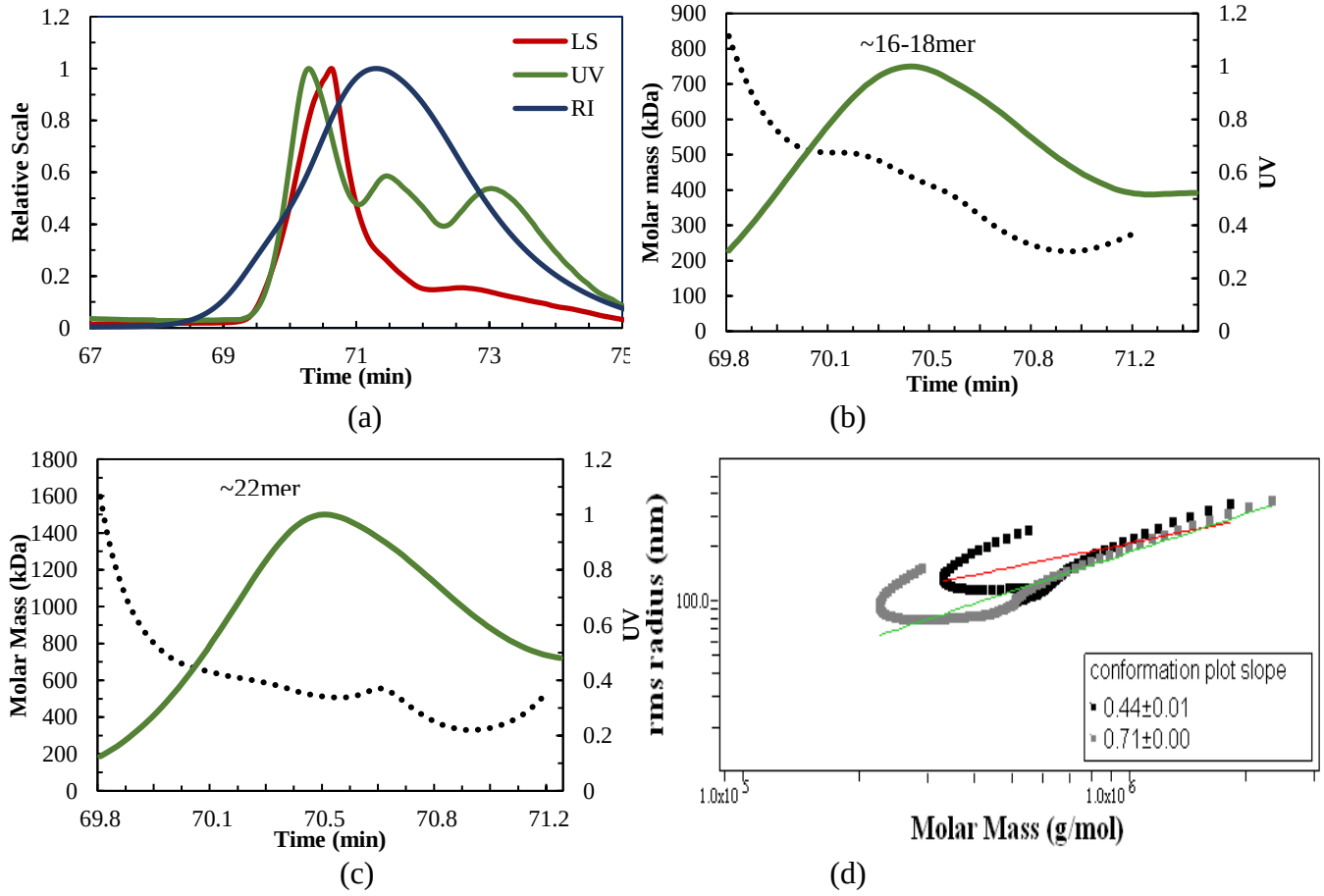

Figure 8. **SEC-MALS of cl-Par-4 in physiological conditions of 0.02 M NaCl** (a) Elution profile of cl-Par-4. (b) and (c) show molar mass (MM) analysis of the major peak from part (a) for two separate runs. (b) M_w (weight average MM -black dots) and UV (green) versus time. The MM at the peak maximum is approximately 424 kilodaltons, consistent with an 18mer. (c) M_w MM plot of a second sample showing a mass of approximately 515 kilodaltons at the peak maximum, consistent with a 22mer. (d) Conformation plot in 0.02 M NaCl for samples shown in (b) and (c). Fitted slopes are 0.44 (black/red) and 0.71 (gray/green).

NaCl [M]	Experimental MM (kDa)	R_g (nm)	Self-association
0.02	389-517	128-155	16.2- 21.6 (16mer-22mer)
1	94	30	3.9 (Tetramer)

Table 1. SEC-MALS in 0.02 and 1 M NaCl

In contrast, for SEC-MALS experiments at 1 M NaCl, smaller oligomers were observed (Figure 9, Table 1). A peak with weak UV intensity eluted after 28-30 minutes, which scattered intensely, consistent with a small amount of aggregation. The largest UV signal came from the second peak which eluted after 40 minutes. This major peak scattered less intensely, which correlates to a smaller species. The average MM for the major peak was 94 kilodaltons which is consistent with tetramer formation (theoretical MM is 96 kilodaltons) (Figure 9b, Table 1).

In total, four samples were run in 1 M NaCl, each with similar results. Within each run (Figure 9b shows the first run), and across the four runs, less variation in MM measurement was observed, indicating a more homogeneous sample than in low salt. However, the slight shoulder on the right edge of the main peak would appear to represent a smaller species such as dimer. This suggests the presence of a small amount of dimer-tetramer interconversion as the sample elutes. The M_w/M_n ratios were approximately 1.05 ± 10% depending on the sample, which is consistent with largely homogeneous samples. Additionally, most of the individual MM measurements had 10% error or below; therefore, we can ascribe tetramer state with some certainty.

The calculated R_g of the tetramer was 30 nm, significantly smaller than the observed R_g of the aggregates. The conformation plot (Figure 9c) has a slope of 0.26, close to 0.33 for spherical proteins. Slopes from additional experiments in high salt include 0.30 and 0.37, which all suggest a mostly spherical protein. Additionally, less sample-to-sample variation in SEC-MALS measurements performed in high salt indicate a more stable structure, with less conformational/associative interconversion evident than at low salt.

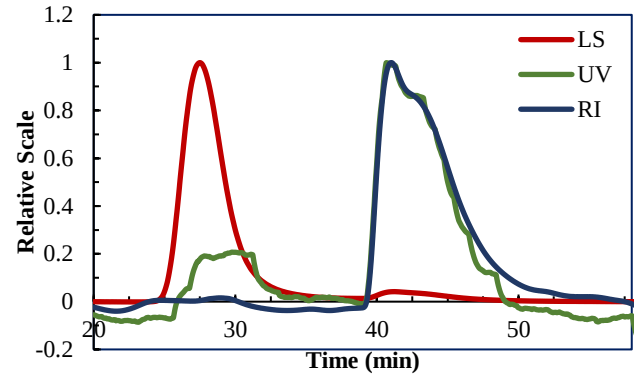

(a)

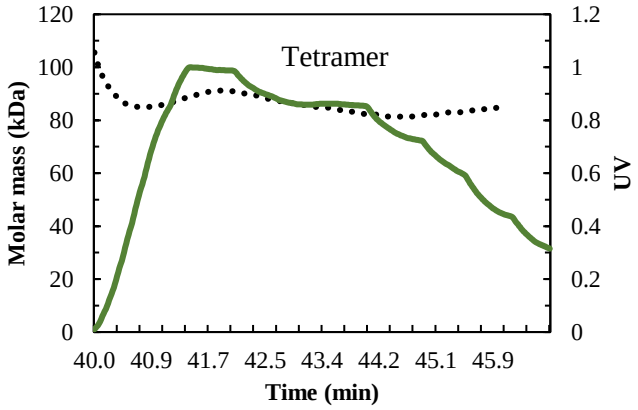

(b)

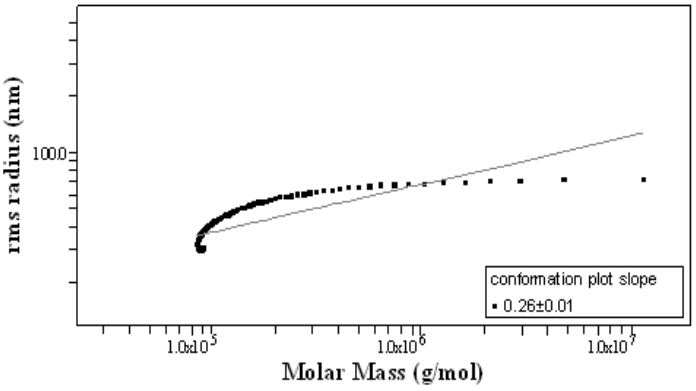

(c)

Figure 9. SEC-MALS of cl-Par-4 in high salt. (a) Elution profile of cl-Par-4 in 1 M NaCl. (b) Plot of molar mass versus time for the major peak shown in (a). The average molar mass is 96 kDa. (c) Conformation plot of rms radius versus molar mass. The slope indicates shape and conformation.

Using GalaxyHomomer modeling software, the YabA tetramer was used as a template to generate a model of the cl-Par-4 tetramer [18, 19]. In the cl-Par-4 tetramer model, each parallel oriented dimer pair (AB and A'B') resembles a pair of tweezers formed by the CC domains, and the two tweezers interact in a scissors-like fashion to form an anti-parallel tetramer (Figure 10).

The SAC and linker domains are shown as mostly helical, but extending away from the coiled coil. They could instead be folded back towards the geometrical center of the tetramer, which would result in a more compact spherical shape.

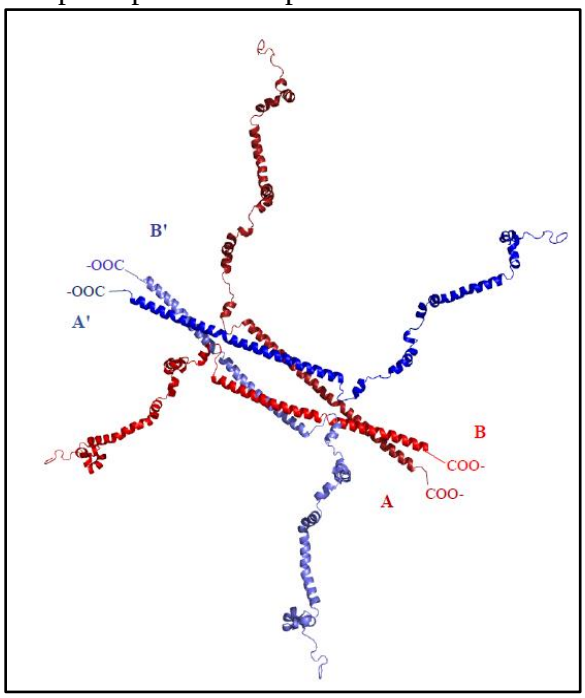

Figure 10. GalaxyHomomer model of cl-Par-4 tetramer.

III. Site-directed mutagenesis of cl-Par-4

Based on the above data, acidic pH and high salt likely promote folding and stability of cl-Par-4 by eliminating charge-charge repulsion in the leucine zipper domain. Figure 11 shows aspartic (D) and glutamic (E) acid residues in the leucine zipper that are electrostatically repulsion under physiological conditions of low salt and neutral pH. In acidic conditions, these residues are protonated and have no negative charge to repel. In high salt and neutral pH, the residues are un-protonated and have a negative charge. The addition of high salt shields the negative charges from repelling and destabilizing coiled coil formation.

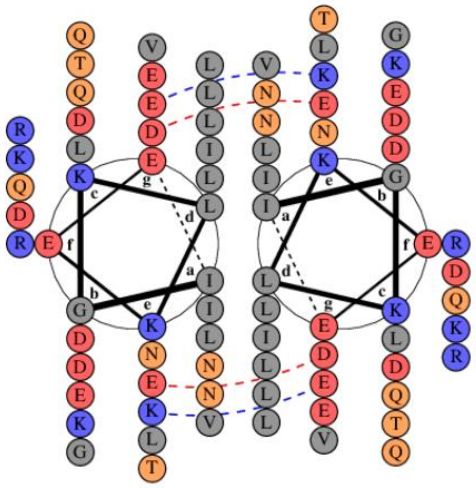

Figure 11. Helical wheel representation of cl-Par-4 dimer leucine zipper domain.

Using site-directed mutagenesis, we are changing the repulsive aspartic and glutamic residues to a positively charged lysine (K). These mutants are D313K and E318K. The replacement of one acidic group with a lysine should create a stabilizing salt bridge. We expect these mutants to have increased stability in physiological conditions and eliminate the need for extreme conditions like high salt or acidic pH.

Primers were designed to insert a lysine in place of the aspartic or glutamic acid residue. Site-directed mutagenesis was performed using the full length Par-4 as a template. DNA samples were sent for sequencing but came back as the wild type, not mutant sequence. The site-directed mutagenesis protocol is currently being optimized to ensure only mutant DNA is obtained and not wild type DNA. The mutants will then be characterized in the same manner as for wild type cl-Par-4.

Conclusion

Our findings have significant implications into understanding why some medically relevant proteins like Par-4 are stable in extreme conditions such as high salt and acidic pH. Electrostatic interactions likely play a role in the folding and stability of cl-Par-4 in extreme conditions and this will be tested via mutagenic analysis. These extreme conditions are often found on extraterrestrial environments and a further understanding of protein folding in extreme conditions will help us understand if proteins and ultimately life itself, could exist in extra-terrestrial environments that do not resemble that of planet Earth.

Acknowledgements

In addition to AMC and SMP, the following authors also contributed to the work presented in this paper: Komala Ponniah, Meghan Warden, Emily Raitt, and Andrea Yawn. The authors wish to thank Professor Vivek Rangnekar, Professor David Libich, and Professor John Cooper, along with Kory Castro and John Bedford.

References

1. El-Guendy, N. and V.M. Rangnekar, *Apoptosis by Par-4 in cancer and neurodegenerative diseases.* Experimental Cell Research, 2003. **283**(1): p. 51-66.
2. Sells, S.F., et al., *Commonality of the Gene Programs Induced by Effectors of Apoptosis in Androgen-dependent and -independent Prostate Cells.* Cell Growth and Differentiation, 1994. **5**: p. 457-466.
3. Libich, D.S., et al., *Intrinsic disorder and coiled-coil formation in prostate apoptosis response factor 4.* The FEBS Journal, 2009. **276**(14): p. 3710-3728.
4. Tompa, P., *Intrinsically unstructured proteins.* Trends in Biochemical Sciences, 2002. **27**(10): p. 527-533.
5. Chaudhry, P., et al., *Prostate Apoptosis Response 4 (Par-4), a Novel Substrate of Caspase-3 during Apoptosis Activation.* Molecular and Cellular Biology, 2012. **32**(4): p. 826-839.
6. El-Guendy, N., et al., *Identification of a Unique Core Domain of Par-4 Sufficient for Selective Apoptosis Induction in Cancer Cells.* Molecular and Cellular Biology, 2003. **23**(16): p. 5516-5525.
7. Sells, S.F., et al., *Expression and function of the leucine zipper protein Par-4 in apoptosis.* Molecular and cellular biology, 1997. **17**(7): p. 3823-3832.
8. Farrand, W.H., et al., *Discovery of jarosite within the Mawrth Vallis region of Mars: Implications for the geologic history of the region.* Icarus, 2009. **204**(2): p. 478-488.
9. Burns, R.G., *Ferric sulfates on Mars.* Journal of Geophysical Research: Solid Earth, 1987. **92**(B4): p. E570-E574.
10. Chen, Y. and E.A. Arriaga, *Individual Acidic Organelle pH Measurements by Capillary Electrophoresis.* Analytical Chemistry, 2006. **78**(3): p. 820-826.
11. Wang, G., et al., *Astrocytes Secrete Exosomes Enriched with Proapoptotic Ceramide and Prostate Apoptosis Response 4 (PAR-4): POTENTIAL MECHANISM OF APOPTOSIS INDUCTION IN ALZHEIMER DISEASE (AD).* Journal of Biological Chemistry, 2012. **287**(25): p. 21384-21395.
12. Kowal, J., M. Tkach, and C. Théry, *Biogenesis and secretion of exosomes.* Current Opinion in Cell Biology, 2014. **29**: p. 116-125.
13. Rothschild, L.J. and R.L. Mancinelli, *Life in extreme environments.* Nature, 2001. **409**: p. 1092.
14. Rampelotto, P.H., *Extremophiles and extreme environments.* Life (Basel, Switzerland), 2013. **3**(3): p. 482-485.
15. Clark, A.M., et al., *pH-Induced Folding of the Caspase-Cleaved Par-4 Tumor Suppressor: Evidence of Structure Outside of the Coiled Coil Domain.* Biomolecules, 2018. **8**(4): p. 162.
16. Alexandrov, A., K. Dutta, and S.M. Pascal, *MBP Fusion Protein with a Viral Protease Cleavage Site: One-Step Cleavage/Purification of Insoluble Proteins.* BioTechniques, 2001. **30**(6): p. 1194-1198.
17. Rollings, J.E., *Use of on-line laser light scattering coupled to chromatographic separations for the determination of molecular weight, branching, size and shape distributions of polysaccharides.* Laser light scattering in biochemistry. Royal Society of Chemistry, Cambridge, UK, 1992: p. 275-293.
18. Ko, J., et al., *GalaxyWEB server for protein structure prediction and refinement.* Nucleic Acids Research, 2012. **40**(W1): p. W294-W297.
19. Felicori, L., et al., *Tetramerization and interdomain flexibility of the replication initiation controller YabA enables simultaneous binding to multiple partners.* Nucleic acids research, 2016. **44**(1): p. 449-463.